HHS Public Access

Author manuscript

*J Endocrinol*. Author manuscript; available in PMC 2021 April 01.

Published in final edited form as:

*J Endocrinol*. 2020 April ; 245(1): 165–178. doi:10.1530/JOE-19-0321.

# Effects of ERβ and ERα on OVX-induced changes in adiposity and insulin resistance

**Terese M. Zidon**[1], **Jaume Padilla**[1,2], **Kevin L. Fritsche**[1], **Rebecca J. Welly**[1], **Leighton T. McCabe**[1], **Olivia E. Stricklin**[1], **Aaron Frank**[3], **Youngmin Park**[1,4], **Deborah J. Clegg**[5], **Dennis B. Lubahn**[6], **Jill A. Kanaley**[1], **Victoria J. Vieira-Potter**[1]

[1]Department of Nutrition and Exercise Physiology, University of Missouri, Columbia MO 65211

[2]Dalton Cardiovascular Research Center, University of Missouri, Columbia MO

[3]Department of Biomedical Sciences, Diabetes and Obesity Research Institute, Cedars-Sinai Medical Center, Los Angeles, California 90048

[4]Department of Exercise and Health Science, Incheon National University, South Korea

[5]College of Nursing and Health Professions, Drexel University, Philadelphia, PA

[6]Dept of Biochemistry, University of Missouri, Columbia, MO

## Abstract

Loss of ovarian hormones leads to increased adiposity and insulin resistance (IR), increasing the risk for cardiovascular and metabolic diseases. The purpose of this study was to investigate whether the molecular mechanism behind the adverse systemic and adipose tissue-specific metabolic effects of ovariectomy requires loss of signaling through estrogen receptor alpha (ERα) or estrogen receptor β (ERβ). We examined ovariectomized (OVX) and ovary-intact wildtype (WT), ERα-null (αKO), and ERβ-null (βKO) female mice (age ~49 weeks; n=7–12/group). All mice were fed a phytoestrogen-free diet (<15 mg/kg) and either remained ovary-intact (INT) or were OVX and followed for 12 weeks. Body composition, energy expenditure, glucose tolerance, and adipose tissue gene and protein expression were analyzed. INT αKO were ~25% fatter with reduced energy expenditure compared to age-matched INT WT controls and βKO mice (all $p<0.001$). Following OVX, αKO mice did not increase adiposity or experience a further increase in IR, unlike WT and βKO, suggesting that loss of signaling through ERα mediates OVX-induced metabolic dysfunction. In fact, OVX in αKO mice (i.e., signaling through ERβ in the absence of ERα) resulted in reduced adiposity, adipocyte size, and IR ($p<0.05$ for all). βKO mice responded adversely to OVX in terms of increased adiposity and development of IR. Together, these findings challenge the paradigm that ERα mediates metabolic protection over ERβ in all settings. These findings lead us to suggest that, following ovarian hormone loss, ERβ may mediate protective metabolic benefits.

**Corresponding author**: Victoria J. Vieira-Potter, Ph. D., 204 Gwynn Hall, University of Missouri, Columbia, MO 65211, vieirapotterv@missouri.edu Ph: 573-882-2027 Fax: 573-884-4885.

**Declaration of interest:** There is no conflict of interest that could be perceived as prejudicing the impartiality of the research reported.

**Keywords**

menopause; metabolism; glucose metabolism; estrogen receptors; adipose tissue

## INTRODUCTION

Estrogen (17β-estradiol [$E_2$]) deficiency in menopausal women and ovariectomized (OVX) rodents is associated with reduced energy expenditure, metabolic disturbances (i.e., insulin resistance [IR]), increased adiposity, and white adipose tissue (WAT) dysfunction (Bluher 2009, 2013; Lovejoy, et al. 2008; Vieira Potter, et al.; Vieira-Potter, et al. 2015). Thus, $E_2$ deficiency increases the risk for developing obesity-related cardiovascular and metabolic diseases, such as type 2 diabetes (Razmjou, et al. 2016; Stefanska, et al. 2015). $E_2$ signaling occurs primarily via the classical genomic pathway through nuclear receptors, estrogen receptor alpha (ERα) and beta (ERβ) (Barros and Gustafsson 2011; Nilsson, et al. 2001). There is mounting evidence that a relationship exists between ERα expression and WAT function in both humans and rodents (Lizcano and Guzman 2014; Monteiro, et al.; Nilsson, et al. 2007b). Young female knockout mice lacking ERα (αKO) have increased adiposity, impaired glucose tolerance (Heine, et al.), and increased WAT inflammation (Ribas, et al.); whereas mice with functional ERα, but not ERβ (βKO), at least prior to OVX, do not show this adverse phenotype (Ohlsson, et al. 2000). Thus, ERα appears critical for providing protection against systemic metabolic and adipose dysfunction prior to OVX. However, whether this dichotomy noted in young ovary-intact females also occurs in older OVX females has not been adequately studied. Davis et al. (Davis, et al.) examined the specific effects of ERα in visceral WAT by selective deletion via viral knockdown of ERα to a single perigonadal fat pad *in vivo* and reported increased adipocyte size and WAT inflammation compared to the untreated fat pad of the same animals. Those data in particular provide strong evidence that $E_2$ signaling via ERα in WAT is required for WAT immune and metabolic health. Moreover, recent data indicate that direct application of $E_2$ on 3T3-L1 adipocytes induces translocation of ERα, but not ERβ, from the nucleus to the plasma membrane (Campello, et al. 2017), which associated with enhanced insulin-stimulated phosphorylation of Akt and GLUT4 translocation. These effects were mimicked by PPT (4,4',4"-(4-Propyl-[1H]-pyrazole-1,3,5-triyl)trisphenol), an ERα agonist, and were blocked by the ERα antagonist, MPP (1,3-Bis(4-hydroxyphenyl)-4-methyl-5-[4-(2-piperidinylethoxy)phenol]-1H-pyrazole dihydrochloride), suggesting that ERα signaling directly affects adipocyte insulin signaling (Campello et al.). Insulin sensitivity of adipose tissue is critical to whole body glucose regulation, particularly among women and older individuals who have a greater relative abundance of adipose tissue. However, insulin sensitivity of adipose tissue also enhances efficient energy storage. Thus, when combined with a state of low total energy expenditure, as is observed following OVX in rodents and menopause in humans, this may increase obesity susceptibility.

$E_2$ supplementation (i.e., hormone replacement therapy [HRT]) has been shown to attenuate weight gain and improve glucose tolerance in both postmenopausal women (Musatov, et al.; Ryan, et al.) and OVX rodents (Stubbins, et al. ; Xu, et al.). Prior studies investigating the role of skeletal muscle showed that $E_2$ directly lowers hepatic glucose production

presumably due to greater glucose uptake into muscle via activation of Akt and induction of GLUT4 expression (Gorres, et al. 2011; Moreno, et al. 2010). On the other hand, liver-specific knock down of ERα increases hepatic glucose production leading to hyperglycemia (Bryzgalova, et al. 2006; Qiu, et al. 2017). Recently, we found that liver expression of ERα is *required* for optimal metabolic improvements following exercise (Winn, et al. 2019). A recent study further showed that $E_2$'s ability to suppress hepatic glucose output requires its ability to suppress Foxo1 via a mechanism involving ERα and activation of Akt (Yan, et al. 2019). Unfortunately, clinical evidence suggests that HRT increases cardiovascular risks (i.e., stroke) in postmenopausal women (Nelson, et al. 2012; Sood, et al.) and is generally not prescribed. Since the detrimental cardiovascular and cancer-provoking effects of HRT are likely mediated through ERα (Drew, et al. 2015; Justenhoven, et al. 2012), therapeutic strategies that target the beneficial effects of $E_2$ but do not activate ERα are necessary to reduce metabolic disturbances seen in this population. Here, we tested the systemic and tissue-specific metabolic effects of OVX in aged female mice null for either ERα or ERβ to assess how adipose tissue $E_2$ signaling via these predominant receptors affects metabolic health following ovarian hormone loss. We hypothesized that, in the setting of advanced age, adipose tissue ERβ signaling would play a *protective* role against OVX-induced weight gain. As such, we predicted that ERβ-null mice would respond more adversely to OVX compared to WT and ERα-null mice. The results support that hypothesis.

## METHODS

### Study design

Randomly cycling female (*Mus musculus* on C57BL/6J background) αKO and βKO mice (N=7–12/group) were pair-housed in a thermoneutral environment (26–28°C) on a 12-hr light/ 12-hr dark cycle. ERα wildtype (WT) controls were used to validate replication of previous studies (Davis et al.; Naaz, et al.) and underwent all treatments similar to the αKO and βKO mice. All mice were initially provided with a low phytoestrogen content (i.e., "washout") diet (150–250 mg/kg; #2018, Teklad Diets; Madison, WI) and water *ad libitum*. One week post-OVX, mice were placed on a phytoestrogen-free (<15 mg/kg phytoestrogens) diet purchased from Harlan Laboratories Inc. (Madison, WI). Body weight (BW) and food intake were monitored and recorded weekly. Ovary-intact (INT) WT, αKO, and βKO mice were examined as separate cohorts serving as INT control groups; these animals did not undergo OVX surgery but were age-matched to represent the "Pre-OVX" condition. For OVX mice, assessments (other than endpoints taken after sacrifice) were made prior to OVX, in addition to 12 weeks post-OVX. At the study conclusion, tissues were harvested from all animals for further analyses as described below. National Institutes of Health guidelines were strictly followed and all procedures were approved by the Institutional Animal Care and Use Committee at the University of Missouri prior to study initiation. αKO mice have been validated to not have functional ERα whereas βKO mice have been validated to exhibit functional ERα (i.e., ERα positive) (Lubahn, et al. 1993). The overall study design is provided in Figure 1.

### Ovariectomy surgeries

For ovariectomy (OVX) surgery, mice (~49 weeks old) were anesthetized and maintained under 2% isoflurane. A single 1 cm dorsal midline incision was made in the skin along the mid-lumbar region followed by two bilateral muscular incisions to expose the ovaries. OVX included removal of the whole ovary, ovarian bursa and part of the oviduct. After ovary removal, the skin incision was closed using skin sutures (4–0 Vicryl; Ethicon) and adhesive (3M VetBond Tissue Adhesive). Buprenorphine (Patterson Veterinary, Devens, MA) was administered subcutaneously at a dose of 0.05 mg/kg immediately after surgery and post-operatively as needed. OVX effectiveness was determined at the conclusion of the study via verification of uterine atrophy; uterine weights are provided herein for INT and OVX WT, αKO, and βKO.

### Body composition

Body fat and lean mass were measured by a non-invasive nuclear magnetic resonance imaging whole-body composition analyzer (EchoMRI® 4in1/1100; Echo Medical Systems, Houston, TX) as previously described (Clookey, et al. 2018). EchoMRI® was performed on conscious mice (N=7–12/ group) to gather pre-surgery data (week 0), mid-way through the study (week 7), and one day prior to sacrifice (12 weeks).

### Glucose tolerance and surrogate markers of insulin resistance

An intraperitoneal glucose tolerance test (GTT) was performed on INT mice and at 8 weeks post-OVX for the OVX groups, as previously described (Vieira-Potter et al. 2015; Wainright, et al. 2015). Briefly, following a six-hour fast, baseline blood (time 0) was collected from a nick in the tail vein and sampled by a hand-held glucometer (AlphaTRAK; Abott Laboratories, Abbott Park, IL). Then, an intraperitoneal injection of a sterile solution of 50% dextrose (2 g/kg BW) was administered. Blood glucose measurements were taken at 15, 30, 45, 60, and 120 minutes following injection. Glucose area under the curve (AUC) above baseline was calculated. Homeostasis model assessment of IR (HOMA-IR) and adipocyte-IR (Adipo-IR) were used as surrogate measures of IR (Matthews, et al. 1985; Sondergaard, et al. 2017) and calculated using the following equations: HOMA-IR [fasting insulin (ng/mL) × fasting glucose (mg/dL)/405] and Adipo-IR [fasting insulin (ng/mL) × NEFA (mmol/L)].

### Indirect calorimetry and physical activity

Indirect calorimetry with a multidimensional beam break monitoring system (Promethion, Sable Systems International, Las Vegas, NV) was used to assess total energy expenditure (TEE), resting energy expenditure (REE), and spontaneous physical activity (SPA) for ovary-intact and 10 weeks post-OVX mice. This system captures synchronized metabolic and behavioral information using a shared gas analyzer chain which pairs individual metabolic cage units with their own flow generator and gas analyzer. Manufacturer-constructed data analysis macros (Expedata Software, Sable Systems International) were used to gather averaged 12-hr light or 12-hr dark cycles. Animals were singly housed in the monitoring system and were allowed to acclimate to the environment 24 hours prior to data collection. SPA was calculated as the sum of the X, Y, and Z beam breaks. TEE and REE are

presented as kcals/kg BW/12-hour cycle as indicated in the figures. Because light REE is most reflective of true resting conditions, we chose to report light cycle REE and dark cycle TEE.

### Fasting circulating markers

Blood was collected upon sacrifice via cardiac puncture and placed into 2.0 mL 7.5% EDTA-treated microcentrifuge tubes (Covidien Monoject). The tubes were then centrifuged to obtain plasma, which was stored in the −80°C freezer until further analysis. Commercial assays for fasting insulin, glucose, cholesterol, triglycerides (TG), low and high density lipoproteins (LDL, HDL) and non-esterified fatty acids (NEFA) were performed by a diagnostic laboratory (Comparative Clinical Pathology Services, Columbia, MO) on an Olympus AU680 automated chemistry analyzer (Beckman-Coulter, Brea, CA) according to manufacturer's guidelines. Plasma $E_2$ was measured via radioimmunoassay at the Vanderbilt University Medical Center Hormone Assay Analytical Core (Vanderbilt University, Nashville, TN, USA) on KO mice. $E_2$ was measured via ELISA (CalBioTech, El Cajon, CA).

### Histological analyses

Formalin-fixed samples (n=4–5/group) were processed through paraffin embedment, sectioned at 5 μm, and stained with hematoxylin and eosin for morphometric determinates, as previously described (Thyfault, et al. 2009). Sections were examined using an Olympus BX60 photomicroscope (Olympus, Melville, NY) and photographed at 20x magnification with a Spot Insight digital camera (Diagnostic Instruments, Sterling Heights, MI). An investigator, blinded to experimental conditions, collected four fields of view from each sample photograph. A representative photograph from one animal per group was selected. For cell size analysis, ~100 random adipocytes, representing at least four fields of view, were analyzed per animal using ImageJ software (National Institutes of Health, public domain).

### RNA extraction and real-time PCR

Samples were homogenized in a Qiazol solution (Qiagen Catalog #79306) using a tissue homogenizer (TissueLyser LT, Qiagen, Valencia, CA). Total RNA from WAT samples from retroperitoneal (i.e., visceral) and subcutaneous (inguinal region) depots was isolated using the Qiagen's RNeasy Lipid Tissue Kit and assayed using a Nanodrop spectrophotometer (Thermo Scientific, Wilmington, DE) to assess purity and concentration. First-strand cDNA was synthesized from total RNA using the High Capacity cDNA Reverse Transcription kit (Applied Biosystems, Carlsbad, CA). Quantitative real-time PCR was performed as previously described using the ABI StepOne Plus sequence detection system (Applied Biosystems) (Padilla, et al.). Primer sequences were designed using the NCBI Primer Design tool (Primers: IDT, Coralville, IA) (Table 1). A 20-μl reaction mixture containing 10 μl iTaq UniverSYBR Green SMX (BioRad, Hercules, CA) and the appropriate concentrations of gene-specific primers plus 4 μl of cDNA template were loaded in each well of a 96-well plate. All PCR reactions were performed in duplicate. PCR was conducted with thermal conditions as follows: 95ºC for 10 min, followed by 40 cycles of 95ºC for 15 s and 60ºC for 45 s. A dissociation melt curve analysis was performed to verify the specificity of the PCR products. 18S primers were used to amplify the endogenous control product (i.e., HK gene).

mRNA expression values are presented as $2^{\Delta CT}$ whereby ΔCT = HK CT - gene of interest CT; data are expressed as fold difference relative to the respective control group.

### Western blot analysis

Western blotting was performed as previously described (Rector, et al. 2008; Thyfault et al. 2009). WAT samples were pulverized and homogenized in Triton X-100 containing protease and phosphatase inhibitors using a tissue homogenizer (TissueLyser LT, Qiagen). WAT protein homogenates (5 μg protein/sample) and Laemmli buffer were then separated by SDS-PAGE using the Criterion vertical gel electrophoresis cell (BioRad, Hercules, CA), transferred to polyvinylidene difluoride membranes utilizing the Criterion blotter wet tank (BioRad, Hercules, CA), then subsequently blocked overnight at 4°C in 5% non-fat dry milk. PVDF membranes were washed with TBS-T then probed with primary antibodies (1:250–1:2000 in 5% bovine serum) overnight at 4°C. Finally, membranes were washed again with TBS-T then incubated in secondary antibody for 1hr at room temperature. Individual protein bands were quantified via chemiluminesence using the FluoroChem HD2 (AlphaView, version 3.4.0,0) and normalized to total protein. Antibodies were purchased from Cell Signaling (Beverly, MA): GLUT4 (1:1000; #2213), phosphorylated Akt (pAkt) (1:250; #4060), and Akt (1:500; #4691).

### Statistics

Determination of sample size was done via power analysis based on our initial studies using β=0.80 and α=0.05 when determining differences between INT and OVX WT mice on the major outcomes, perigonadal fat pad mass and glucose AUC, which indicated a minimum sample size of 5 and 11, respectively. The sample sizes varied from 7–12/group and are provided in the figure legends. Normality was tested using standard assessments (Kolmogorov-Smirnov and Shapiro-Wilk); p values were all > 0.05 allowing us to determine that the data were normally distributed. Where appropriate, main effects of genotype (WT, αKO, βKO) and OVX (OVX vs. INT) were determined via 2×3 analysis of variance (ANOVA). When a significant genotype x OVX interaction was observed, a *post hoc* Tukey test was used to detect where differences occurred. Post hoc Tukey's tests were used to determine which genotypes differed, and which were affected by OVX, where appropriate. For mRNA expression of the retroperitoneal WAT depot, we were not able to run 2×3 ANOVA because the INT and OVX samples were processed separately and differences in housekeeping gene expression did not allow for INT vs OVX comparison. Thus, we utilized 1-way ANOVA within each condition (i.e., INT and OVX) followed by *post hoc* Tukey's where appropriate for those analyses. Data were analyzed using SPSS v24 (Chicago, IL) and are presented as mean ± SEM where p≤0.05 was considered statistically significant.

## RESULTS

### Genotype-specific body composition changes following OVX

INT αKO mice weighed ~25% more than WT and βKO controls (Figure 2A; p<0.01), whereas βKO and WT did not differ. Following OVX, weight differences no longer existed because both WT (+25%) and βKO (+31%) mice demonstrated a significant increase in body mass compared to their respective pre-OVX body weights, while αKO did not change;

thus, WT and βKO had significantly greater OVX-associated body weight gain than αKO (Figure 2B, $p<0.01$). These body weight differences were due to differences in adiposity; INT αKO mice had significantly greater percent fat mass than WT and βKO ($p<0.01$) (Figure 2C). Similarly, percent fat increased in both WT (+66%) and βKO (+60%) following OVX (both $p<0.05$); while, it did not increase in αKO (−9%) (NS) (Figure 2C). This resulted in OVX-associated body fat increases only in the WT and βKO (Figure 2D), whereas, αKO moved in the opposite direction following OVX. Similarly, following OVX, βKO had significantly lower percent lean mass than αKO due to reductions in percent lean mass in WT (−16%; $p<0.05$) and βKO (−18%; $p<0.05$) and non-significant gain in the αKO (+8%) (NS) (data not shown),.

Visceral adiposity (i.e., assessed here via perigonadal fat pad weights, Figure 3A; and mean adipocyte size, Figure 3B-C) between the INT groups did not differ. Following OVX, visceral adiposity of αKO did not change ($p=0.89$), whereas WT ($p=0.02$) and βKO ($p=0.015$) both experienced OVX-induced increases, resulting in lower visceral adiposity in αKO compared to the other groups. Representative histological images of perigonadal adipose tissue reflect these differences, revealing that adipocyte size only increased following OVX in the WT and βKO groups (Figure 3C).

## Genotype-specific differences in white adipose tissue gene expression

White adipose tissue (WAT) from subcutaneous and visceral (from retroperitoneal region) depots were assessed for inflammatory cytokines, adipokines, and markers of mitochondrial activity and endocrine function. Interestingly, in the INT state, mRNA expression of the insulin-sensitizing adipokine, adiponectin in the retroperitoneal WAT was ~3-fold higher in the βKO mice compared to WT and αKO mice (Figure 4A; $p<0.001$), whereas leptin expression was not different between genotypes. This resulted in the adiponectin to leptin ratio to be higher in the βKO compared to the αKO mice ($p=0.04$). In addition, gene expression of the inflammatory macrophage marker, CD11c was increased in both αKO and βKO compared to WT (both $p<0.05$ compared to WT). Unfortunately, due to timing differences of mRNA isolation resulting in housekeeping gene differences between INT and OVX mice, we were not able to compare INT to OVX gene expression for this WAT depot. Among OVX groups, no statistically significant differences were observed between groups (Figure 4B). Thus, the increase in adiponectin gene expression in βKO was dependent on ovarian status (i.e., only observed in the INT state).

In examining mRNA differences in subcutaneous WAT across INT and OVX groups, no significant differences were observed. Since we had sufficient tissue in this depot, we also analyzed aromatase and uncoupling protein 1 (UCP1) gene expression (we were not able to measure these in the retroperitoneal depot due to insufficient tissue). No differences between groups were observed. Insulin signaling proteins, IRS1 and GLUT4 were both reduced by OVX independent of genotype (main effect of OVX, $p<0.05$ for both genes) (Figure 4C).

## Genotype-specific changes in indicators of insulin resistance following OVX

GTT curves are presented for INT (Figure 5A) and OVX states (Figure 5B) across the three genotypes. While both WT and βKO experienced an OVX-induced increase in GTT glucose

area under the curve (AUC), this was not observed in αKO mice (Figure 5C, genotype x OVX $p<0.05$). Similarly, the surrogate indices of insulin resistance, HOMA-IR (Figure 5D) and Adipo-IR (Figure 5E), both increased following OVX in the WT and βKO mice, but *decreased* in the αKO (all genotype x OVX interactions, $p<0.05$). In comparing genotypes in the INT state for basal insulin signaling in WAT (subcutaneous depot), as determined by phosphorylated Akt (i.e., pAKT relative to total Akt), βKO had significantly higher levels of pAKT compared to both WT and βKO (Figure 5F; $p<0.001$). However, following OVX, whereas both αKO and WT experienced increases in pAKT, βKO did not change (genotype x OVX interaction, $p<0.05$). There were no differences across OVX groups for GLUT4 protein in the basal/fasting condition, indicating that the apparent greater basal insulin stimulation (reflected by pAkt) did not result in increased glucose uptake into WAT (Figure 5G).

Fasting blood biochemistry, including blood lipids, are provided in Table 2. Coinciding with their glucose intolerance, INT αKO mice had higher levels of fasting insulin compared to WT (non-significant trend, $p=0.12$) and βKO mice ($p=0.043$); βKO mice were similar to WT. As far as blood lipids, the only significant differences that were observed were for the βKO mice, who experienced increases in total, HDL, and LDL cholesterol with OVX compared to the INT state (all $p<0.05$). Thus, OVX βKO mice had significantly greater total and LDL cholesterol than OVX WT mice (both $p<0.05$). Circulating levels of $E_2$ were not different than INT WT and βKO, and αKO mice had significantly higher estradiol levels than the other groups ($p<0.05$), which is typical for this model (Islander, et al. 2003). Liver mass and triglyceride content were evaluated as additional indirect indicators of insulin sensitivity and overall metabolic health. Liver mass was not different based on genotype ($p=0.234$) or OVX state ($p=0.716$), yet liver TG content was almost twice as high in the βKO compared to WT and αKO ($p<0.05$); OVX did not significantly affect liver TG content in either genotype ($p=0.218$). As included inTable 2, ovarian mass differences validated successful OVX surgery in all genotypes ($p<0.001$).

### Genotype-specific changes in energy expenditure and s physical activity following OVX

INT αKO mice had significantly lower total energy expenditure (TEE) compared to age-matched WT in both the 12-hour light (inactive) and dark (active) cycles (dark cycle shown, Figure 6A; $p<0.05$). βKO mice were not different from WT controls in either cycle. These differences coincided with similar differences in resting energy expenditure (REE) (Figure 6B; $p<0.05$). Spontaneous physical activity (SPA) during the dark cycle tended to be lower in αKO (Figure 6C; $p=0.052$). These data confirm what has been demonstrated in previous studies using younger αKO mice compared to their WT littermates (Heine et al. 2000; Naaz et al. 2002). Following OVX, WT experienced a reduction in SPA ($p<0.05$) but βKO and αKO did not significantly change; this resulted in no differences in SPA following OVX among the three genotypes. Comparisons between the INT and OVX state within genotype also revealed significant reductions in TEE during the dark (active) cycle ($p<0.01$) and REE during the light (inactive) cycle ($p<0.01$) in both WT and βKO following OVX, but were not evident in αKO mice following OVX. There were also no differences among the genotypes following OVX in TEE, REE, or food intake (data not shown).

## DISCUSSION

The purpose of the current study was to use age-appropriate mouse models to determine whether the molecular mechanisms for OVX-mediated systemic and WAT-specific metabolic dysfunction require loss of signaling through either ERα or ERβ. In order to investigate which ER is responsible for OVX-mediated metabolic changes, we used aged female WT, whole body αKO, and whole body βKO mice and compared them before (i.e., ovary-intact [INT] state) and after OVX. WAT is a tissue with high expression of both ERα and ERβ (Gao and Dahlman-Wright 2013; Stubbins, et al. 2012b) and estrogen is produced in adipose tissue and modulates adipose tissue metabolism both before and after OVX (Stubbins et al. 2012b). OVX of these ERα and ERβ KO mouse models provides a unique opportunity to investigate the role of adipose tissue local estrogen signaling on metabolic manifestations in the setting of low circulating estrogen. The major findings are that: *(1)* obesity and systemic IR caused by OVX is likely attributed to loss of central signaling through ERα; and *(2)* the presence of ERβ signaling, combined with the absence of ERα signaling in WAT, may play a protective role in preventing OVX-mediated obesity and IR.

First, we compared the WT, αKO, and βKO mice in the INT state at the age that we ovariectomized an additional cohort from each group (i.e., ~49 weeks). This allowed us to gain age-appropriate insight about the effect ovarian hormone loss has on women approaching menopause. We found that these older female αKO mice display phenotypic characteristics of metabolic dysfunction compared to WT controls, similar to those differences previously observed in younger αKO mice (Clookey, et al. 2019; Heine et al. 2000; Ogawa, et al. 2003). Compared to WT, they were obese and displayed IR. The obesity was not driven by differences in food intake (data not shown – no differences), but rather, reduced energy expenditure in the αKO. Further, the reduced energy expenditure was driven by a trend toward lower cage physical activity, as well as lower resting metabolic rate. Although other studies have shown significant differences in spontaneous physical activity between younger WT and αKO mice, our findings of more modest physical activity differences may be explained by age-related reduction in physical activity, as observed in other models. These data confirm that ERα plays a protective metabolic role on systemic health prior to ovarian insufficiency, due in part to its role in increasing energy expenditure. Similarly, as previously shown in younger animals (Clookey et al. 2019; Gao and Dahlman-Wright 2013; Heine et al. 2000), the INT βKO studied here did not display an adverse metabolic profile compared to WT and were not different in indices of obesity, IR, or energy expenditure compared to WT. One exception was that, compared to the αKO, the βKO had greater visceral WAT content, and greater WAT adiponectin gene expression. This may be due to ERβ mediated antagonization of PPARλ. Previously published *in vitro* studies by Foryst-Ludwig and colleagues showed that ERβ inhibits ligand-mediated PPARλ transcriptional activity, which results in abrogation of PPARλ-induced adipocyte proliferation (Foryst-Ludwig, et al. 2008). Other studies support an important relationship between ERβ and PPARλ (Velickovic, et al. 2014; Wang, et al. 2015).

As predicted, OVX did not exacerbate the metabolic phenotype in αKO mice, who exhibited pronounced metabolic dysfunction even in the INT state. However, this group exhibited apparent *reductions* in adiposity and adipocyte size, as well as apparent *improvements* in

insulin sensitivity, indicated predominantly by lower levels of fasting insulin. Others had previously demonstrated that OVX in young αKO mice reduces body weight, visceral adiposity, and glucose intolerance (Naaz et al. 2002); we confirm here that this phenomenon is also true in older animals. This was in stark contrast to WT and βKO mice, who experienced increases in adiposity and IR following OVX. This may implicate ERβ (possibly via ligand activation by local estrogen produced in WAT) as having a protective metabolic role in the setting of low circulating estrogen (e.g., following OVX). Importantly, estrogen production in adipose tissue is the major source of estrogen following OVX, where estrogen signaling in WAT remains or is increased (Iyengar, et al. 2013). Unfortunately, we were not able to measure aromatase in visceral WAT. We were only able to measure aromatase gene expression in subcutaneous WAT, and found no differences in INT or OVX states. Future studies should measure aromatase activity and protein content, and look at depots other than subcutaneous WAT.

It has recently been suggested that the balance between ERα and ERβ protein in the WAT of menopausal women may be an important determinant for estrogen-mediated improvements in WAT insulin sensitivity, such that women with a higher ERα/ERβ ratio respond more robustly to estrogen in terms of adipocyte insulin sensitivity (Shin, et al. 2007; Park, et al. 2017). It has also been reported that a greater density of ERα over ERβ associates with obesity in rodents (Shin et al. 2007), and human studies reveal strong links between polymorphisms in the ESR2 gene (i.e., encoding ERβ) and obesity, whereas polymorphisms in the ESR1 gene (i.e., encoding ERα) do not associate with obesity in humans (Nilsson, et al. 2007a). This may be due to the fact that activation of ERα improves WAT insulin sensitivity, thus facilitating efficient fat storage. On the other hand, activation of ERβ reduces adipogenesis and adiponectin expression, possibly via a mechanism involving inhibition of PPARλ as described above (Foryst-Ludwig et al. 2008), which may help explain its recently documented adiposity-reducing effect (Ponnusamy, et al. 2017a; Sasayama, et al. 2017). This may also explain why INT βKO in the present study had significantly greater WAT adiponectin expression prior to OVX, and tended to gain more adiposity following OVX compared to the other groups. Adiponectin mRNA expression in the visceral WAT of the INT βKO mice was ~3-fold higher compared to both WT and αKO while the adiponectin-to-leptin ratio (indicative of adipocyte insulin sensitivity) was ~2-fold higher compared to αKO mice. Adiponectin is a potent anti-inflammatory and insulin-sensitizing adipokine secreted from the adipose tissue (Yamauchi, et al.). Premenopausal women, who exhibit greater adiposity yet are metabolically protected against metabolic dysfunction compared to age-matched males, secrete greater levels of adiponectin (Kern, et al.). Our data may suggest that ERα signaling is mechanistically responsible for that protective increase in adiponectin. Supporting this, young ERβ-null mice exhibit improved insulin sensitivity despite weight gain, presumably related to their greater adiponectin synthesis (Foryst-Ludwig et al. 2008).

Thus, it appears that most of the insulin-sensitizing effect of estrogen signaling is through ERα. Yet, we show that, following OVX, mice *lacking* ERα (i.e., forcing the majority of the available estrogen to activate ERβ) respond with *improved* insulin sensitivity, adipocyte size, and adiposity. To interrogate potential WAT-specific mechanisms for this paradoxical finding, we investigated insulin signaling genes and proteins in WAT. In the INT state, WAT

protein levels of pAKT relative to total AKT, indication of basal levels of insulin signaling, were greater in the βKO mice compared to WT and αKO mice. Moreover, OVX significantly increased pAKT only in WT and αKO, bringing their levels to that of the INT βKO (Fig. 5F). Although comparisons of pAKT *in response to acute insulin stimulation* may be predicted to be lower in settings of IR, here we only measured basal (i.e., non-insulin stimulated) levels. Thus, these higher levels likely reflect greater IR and greater lipid storage, rather than enhanced glucose clearance. Indeed, these differences did not associate with increases in GLUT4, the insulin-dependent glucose transporter in WAT. In fact, gene expression levels of GLUT and IRS1 were significantly suppressed following OVX, supporting OVX-associated disruption in glucose clearance. Future studies should more precisely measure adipocyte insulin signaling in these models. Although no other studies (to our knowledge) have assessed how OVX affects pAkt in WAT in αKO or βKO mice, cell signaling studies have shown that ERβ mediates Akt activation (Lin, et al. 2017) supporting the hypothesis that ERβ may actually facilitate insulin-stimulated glucose uptake.

Additional research into potential mechanisms by which ERβ signaling affects WAT insulin sensitivity and metabolism is clearly required. These findings raise questions about selective activation of ERα vs. ERβ, particularly following menopause. Previous work has shown that the selective ERα agonist, PPT, in aged OVX mice attenuated weight gain, enhanced insulin sensitivity, and increased energy expenditure compared to controls (Hamilton, et al. 2016) confirming ERα's beneficial role in systemic metabolism in aged mice; however, those authors did not assess ERβ's role. Since selective agonization of ERα is not recommended in postmenopausal women who have an elevated risk for breast cancer, our findings that ERβ may also mediate beneficial effects following hormone loss, has important clinical relevance. In the present study, OVX in both WT and βKO mice (i.e., two genotypes with normal ERα expression) resulted in weight gain via increased adiposity, reduced energy expenditure, and glucose intolerance. However, OVX in βKO mice led to increased IR compared to the INT condition. Together, these data support a possible protective metabolic role for ERβ following OVX.

Since OVX causes WAT inflammation, which precedes the onset of systemic IR (Vieira Potter et al. 2012), and visceral WAT-specific ERα knockdown also increases inflammation (Davis et al. 2013), it seems that loss of ERα would result in increased inflammation. Indeed, gene expression of the inflammatory macrophage marker known to associate with systemic IR, CD11c, was significantly elevated in visceral WAT of INT αKO compared to INT WT. However, and INT βKO also had greater levels compared to WT, suggesting that in aged mice, ERβ may also buffer inflammation (Fig. 4A). Interestingly, INT βKO were unique in having significantly higher visceral WAT adiponectin expression, a difference that diminished following OVX (Fig. 4B). This may have protected the INT βKO from IR (Fig. 5D-E). Although it was surprising that no other differences in inflammatory markers were found in either WAT depot of either genotype, robust increases in WAT inflammation may require chronic high-fat feeding or longer duration following OVX. Or, it may be that all animals experienced age-induced WAT inflammation thus preventing differences between groups from being determined. We also quantified immune cells (i.e., from the stromal vascular fraction) from visceral WAT from a subset of these mice and phenotyped T cells and macrophages – no differences were found, so those data were not included. Future

studies should compare old and younger animals in this regard in order to interrogate aging effects from effects attributed to hormone loss per se.

Although it is tempting to attribute the robust OVX-associated changes observed in WT and βKO mice to reduction in circulating $E_2$, no differences in circulating $E_2$ between INT and OVX βKO or between INT and OVX WT mice were found. There are a few potential explanations for this. One is that the robust adiposity increases in the WT and βKO mice, but not ERα, resulted in increases in extragonadal $E_2$ production (i.e., from adipose tissue), which may have been detected in the circulation. Indeed, high fat diet-induced obesity is known to increase circulating $E_2$ in OVX mice, whereas this obesity-induced $E_2$ increase does not appear to be protective (at least on bone). It is not known if ovarian vs extra-ovarian estrogens have differential effects on metabolism. Additional studies are necessary to further interrogate how ovarian vs. extra-ovarian estrogens affect systemic and adipose tissue metabolism. Another possibility is that ovarian hormones other than $E_2$ may play an important role in OVX-mediated changes, while only $E_2$ was measured here. Future studies should measure testosterone, progesterone, and additional forms of estrogen (e.g., estrone). It may be that the ratio of $E_2$ to these other hormones is more important than total circulating $E_2$, per se. Finally, we did not measure sex hormone binding globulin (SHBG); thus, it may be that OVX increased SHBG, making the level of *bioavailable* $E_2$ much less following OVX; we measured total $E_2$ only. Future studies should thus measure SHBG in addition to other ovarian hormones.

### Strengths and limitations.

Use of older female αKO and βKO mice provided an additional stress not previously investigated in these models following OVX. This approach is more representative of age-related hormonal changes typically observed in women. However, future studies should utilize WAT-specific knock out models to further interrogate the adipose tissue-specific effects of signaling through ERα and ERβ on responses to selective ligands following OVX. We recently demonstrated by adipose tissue-specific activation (i.e., via selective beta 3 adrenergic receptor ligand) completely restored the systemic and adipose tissue metabolic phenotype induced by loss of ERα signaling (Clookey et al. 2019). The role of aging and ovarian hormone state on the potential efficacy of specific ERα versus ERβ ligands requires more intense investigation. Nevertheless, based on our primary findings that (1) “forced” signaling through ERβ (owing to the absence of ERα) results in reductions in adiposity, adipocyte size, and IR following OVX, and (2) suppressed signaling through ERβ exacerbates adiposity gain following OVX, we conclude that selective activation of ERβ may be an important metabolic therapeutic in settings of low circulating estrogen. Previous studies have shown that ERβ-null mice display increased susceptibility to OVX (Seidlova-Wuttke et al. 2012) and we confirm that here. Although mechanisms are not fully understood, accumulating evidence indicates that systemic activation of ERβ reduces adiposity by activating adipocyte mitochondrial activity (Ponnusamy, et al. 2017) 3. We hypothesize that local adipose tissue estrogen may be protective following OVX by activating ERβ and improving mitochondrial activity. On the other hand, activation of ERα may enhance adipocyte insulin sensitivity and facilitate lipid storage.

As summarized in Figure 7, following OVX, a reduction in systemic energy expenditure, driven by reduced central ERα signaling, associates with 'healthy' deposition of adipose tissue due to its high insulin sensitivity, which is attributed largely to ERα signaling in adipose tissue. Thus, in the ovary-intact (and premenopausal) condition, estrogen (via ERα) both increases systemic energy expenditure and enhances adipocyte insulin sensitivity – this leads to a lean and insulin sensitive phenotype. However, following OVX (and menopause), a reduction in centrally mediated energy expenditure combined with high adipocyte insulin sensitivity (due to greater ERα / ERβ signaling in adipose tissue combined with local adipose tissue estrogen production) leads to more efficient fat storage and positive energy balance (i.e., obesity). We hypothesize that a greater ERβ / ERα ratio may offset this by reducing fat storage and adipocyte size. Mechanistically, this may occur via ERβ-mediated increased adipocyte energy expenditure and suppressed adipocyte proliferation. This hypothetical model requires further testing, but support for it would implicate ERβ ligands as potential therapeutics to reduce obesity following menopause. Indeed, recent evidence indicates that activation of ERβ exerts potent anti-obesity effects (Gonzalez-Granillo, et al. 2019; Miao, et al. 2016; Ponnusamy et al. 2017a; Ponnusamy, et al. 2017b; Sasayama et al. 2017). Importantly, unlike ERα, adipose tissue expression of ERβ increases following OVX in the setting of aging (Tomicek, et al. 2011), revealing a window of opportunity to protect postmenopausal women via selective ERβ activation. Another important fact to note is that the metabolic actions of ERα are mediated through two distinct activation functions – AF1 and AF2. In 2017, Guillaume et al. demonstrated that the effects of tamoxifen (used to activate ERα in specific tissues) to protect against IR and obesity requires AF1 but not AF2 (Guillaume, et al. 2017). Our studies cannot distinguish which aspects of ERα (and/or ERβ) signaling were responsible for the differential effects following OVX but future studies should determine the specific receptor mediated mechanisms. Finally, a critical adverse consequence of menopause is reduced bone density due to the decline in circulating estrogens, and reduction in estrogen/ER-mediated effects are largely responsible for this. This has been shown in OVX animals and postmenopausal women. Thus, an important future direction is to determine the role of reduced ER signaling on bone-specific responses to OVX. In conclusion, the findings presented here lead us to suggest that the systemic metabolic effects of OVX are mediated through central loss of ERα signaling, while the activation of ERβ in adipose tissue by locally produced estrogen may be protective. Thus, ERβ may be an attractive therapeutic target to improve metabolism following ovarian hormone loss.

## ACKNOWLEDGEMENTS

Funded by: MU-CBIS pilot grant (NCCAM/ODS/NCI #P50AT006273) and MU Research Council to V. Vieira-Potter; MU-CAB (T.M.Z). J.P. was supported by NIH K01 HL-125503. Mice were generously donated by D.B. Lubahn, Ph.D. from the University of Missouri. The VUMC Hormone Assay and Analytical Services Core is supported by NIH grants DK059637 and DK020593. We would like to thank Makenzie L. Woodford for her assistance in carrying out some of the experiments performed as a part of this study.

## REFERENCES

Barros RP & Gustafsson JA 2011 Estrogen receptors and the metabolic network. Cell Metab 14 289–299. [PubMed: 21907136]

Bluher M 2009 Adipose tissue dysfunction in obesity. Exp Clin Endocrinol Diabetes 117 241–250. [PubMed: 19358089]

Bluher M 2013 Adipose tissue dysfunction contributes to obesity related metabolic diseases. Best Pract Res Clin Endocrinol Metab 27 163–177. [PubMed: 23731879]

Brown LM, Clegg DJ. Central effects of estradiol in the regulation of food intake, body weight, and adiposity. J Steroid Biochem Mol Biol. 2010;122(1–3):65–73. [PubMed: 20035866]

Bryzgalova G, Gao H, Ahren B, Zierath JR, Galuska D, Steiler TL, Dahlman-Wright K, Nilsson S, Gustafsson JA, Efendic S, et al. 2006 Evidence that oestrogen receptor-alpha plays an important role in the regulation of glucose homeostasis in mice: insulin sensitivity in the liver. Diabetologia 49 588–597. [PubMed: 16463047]

Campello RS, Fatima LA, Barreto-Andrade JN, Lucas TF, Mori RC, Porto CS & Machado UF 2017 Estradiol-induced regulation of GLUT4 in 3T3-L1 cells: involvement of ESR1 and AKT activation. J Mol Endocrinol 59 257–268. [PubMed: 28729437]

Cao JJ, Gregoire BR. A high-fat diet increases body weight and circulating estradiol concentrations but does not improve bone structural properties in ovariectomized mice. Nutr Res. 2016;36(4):320–327. [PubMed: 27001277]

Clookey SL, Welly RJ, Shay D, Woodford ML, Fritsche KL, Rector RS, Padilla J, Lubahn DB & Vieira-Potter VJ 2019 Beta 3 Adrenergic Receptor Activation Rescues Metabolic Dysfunction in Female Estrogen Receptor Alpha-Null Mice. Front Physiol 10 9. [PubMed: 30804793]

Clookey SL, Welly RJ, Zidon TM, Gastecki ML, Woodford ML, Grunewald ZI, Winn NC, Eaton D, Karasseva NG, Sacks HS, et al. 2018 Increased susceptibility to OVX-associated metabolic dysfunction in UCP1-null mice. J Endocrinol.

Davis KE, M DN, Sun K, W MS, J DB, J AZ, Zeve D, L DH, D WC, L MG, et al. 2013 The sexually dimorphic role of adipose and adipocyte estrogen receptors in modulating adipose tissue expansion, inflammation, and fibrosis. Mol Metab 2 227–242. [PubMed: 24049737]

Drew BG, Hamidi H, Zhou Z, Villanueva CJ, Krum SA, Calkin AC, Parks BW, Ribas V, Kalajian NY, Phun J, et al. 2015 Estrogen receptor (ER)alpha-regulated lipocalin 2 expression in adipose tissue links obesity with breast cancer progression. J Biol Chem 290 5566–5581. [PubMed: 25468909]

Foryst-Ludwig A, Clemenz M, Hohmann S, Hartge M, Sprang C, Frost N, Krikov M, Bhanot S, Barros R, Morani A, et al. 2008 Metabolic actions of estrogen receptor beta (ERbeta) are mediated by a negative cross-talk with PPARgamma. PLoS Genet 4 e1000108.

Gao H & Dahlman-Wright K 2013 Implications of estrogen receptor alpha and estrogen receptor beta for adipose tissue functions and cardiometabolic complications. Horm Mol Biol Clin Investig 15 81–90.

Gonzalez-Granillo M, Savva C, Li X, Fitch M, Pedrelli M, Hellerstein M, Parini P, Korach-Andre M & Gustafsson JA 2019 ERbeta activation in obesity improves whole body metabolism via adipose tissue function and enhanced mitochondria biogenesis. Mol Cell Endocrinol 479 147–158. [PubMed: 30342056]

Gorres BK, Bomhoff GL, Morris JK & Geiger PC 2011 In vivo stimulation of oestrogen receptor alpha increases insulin-stimulated skeletal muscle glucose uptake. J Physiol 589 2041–2054. [PubMed: 21486807]

Guillaume M, Handgraaf S, Fabre A, Raymond-Letron I, Riant E, Montagner A, Vinel A, Buscato M, Smirnova N, Fontaine C, et al. 2017 Selective Activation of Estrogen Receptor alpha Activation Function-1 Is Sufficient to Prevent Obesity, Steatosis, and Insulin Resistance in Mouse. Am J Pathol 187 1273–1287. [PubMed: 28502695]

Hamilton DJ, Minze LJ, Kumar T, Cao TN, Lyon CJ, Geiger PC, Hsueh WA & Gupte AA 2016 Estrogen receptor alpha activation enhances mitochondrial function and systemic metabolism in high-fat-fed ovariectomized mice. Physiol Rep 4.

Heine PA, Taylor JA, Iwamoto GA, Lubahn DB & Cooke PS 2000 Increased adipose tissue in male and female estrogen receptor-alpha knockout mice. Proc Natl Acad Sci U S A 97 12729–12734. [PubMed: 11070086]

Islander U, Erlandsson MC, Hasseus B, Jonsson CA, Ohlsson C, Gustafsson JA, Dahlgren U & Carlsten H 2003 Influence of oestrogen receptor alpha and beta on the immune system in aged female mice. Immunology 110 149–157. [PubMed: 12941152]

Iyengar NM, Hudis CA & Dannenberg AJ 2013 Obesity and inflammation: new insights into breast cancer development and progression. Am Soc Clin Oncol Educ Book 46–51. [PubMed: 23714453]

Justenhoven C, Obazee O & Brauch H 2012 The pharmacogenomics of sex hormone metabolism: breast cancer risk in menopausal hormone therapy. Pharmacogenomics 13 659–675. [PubMed: 22515609]

Kern PA, Di Gregorio GB, Lu T, Rassouli N & Ranganathan G 2003 Adiponectin expression from human adipose tissue: relation to obesity, insulin resistance, and tumor necrosis factor-alpha expression. Diabetes 52 1779–1785. [PubMed: 12829646]

Lin KH, Kuo WW, Shibu MA, Day CH, Hsieh YL, Chung LC, Chen RJ, Wen SY, Viswanadha VP & Huang CY 2017 E2/ER beta Enhances Calcineurin Protein Degradation and PI3K/Akt/MDM2 Signal Transduction to Inhibit ISO-Induced Myocardial Cell Apoptosis. Int J Mol Sci 18.

Lizcano F & Guzman G 2014 Estrogen deficiency and the origin of obesity during menopause. Biomed Res Int 2014 757461.

Lovejoy JC, Champagne CM, de Jonge L, Xie H & Smith SR 2008 Increased visceral fat and decreased energy expenditure during the menopausal transition. Int J Obes (Lond) 32 949–958. [PubMed: 18332882]

Lubahn DB, Moyer JS, Golding TS, Couse JF, Korach KS & Smithies O 1993 Alteration of reproductive function but not prenatal sexual development after insertional disruption of the mouse estrogen receptor gene. Proc Natl Acad Sci U S A 90 11162–11166. [PubMed: 8248223]

Matthews DR, Hosker JP, Rudenski AS, Naylor BA, Treacher DF & Turner RC 1985 Homeostasis model assessment: insulin resistance and beta-cell function from fasting plasma glucose and insulin concentrations in man. Diabetologia 28 412–419. [PubMed: 3899825]

Miao YF, Su W, Dai YB, Wu WF, Huang B, Barros RP, Nguyen H, Maneix L, Guan YF, Warner M, et al. 2016 An ERbeta agonist induces browning of subcutaneous abdominal fat pad in obese female mice. Sci Rep 6 38579.

Monteiro R, Teixeira D & Calhau C 2014 Estrogen signaling in metabolic inflammation. Mediators Inflamm 2014 615917.

Moreno M, Ordonez P, Alonso A, Diaz F, Tolivia J & Gonzalez C 2010 Chronic 17beta-estradiol treatment improves skeletal muscle insulin signaling pathway components in insulin resistance associated with aging. Age (Dordr) 32 1–13. [PubMed: 19462258]

Musatov S, Chen W, Pfaff DW, Mobbs CV, Yang XJ, Clegg DJ, Kaplitt MG & Ogawa S 2007 Silencing of estrogen receptor alpha in the ventromedial nucleus of hypothalamus leads to metabolic syndrome. Proc Natl Acad Sci U S A 104 2501–2506. [PubMed: 17284595]

Naaz A, Zakroczymski M, Heine P, Taylor J, Saunders P, Lubahn D & Cooke PS 2002 Effect of ovariectomy on adipose tissue of mice in the absence of estrogen receptor alpha (ERalpha): a potential role for estrogen receptor beta (ERbeta). Horm Metab Res 34 758–763. [PubMed: 12660895]

Nelson HD, Walker M, Zakher B & Mitchell J 2012 Menopausal hormone therapy for the primary prevention of chronic conditions: a systematic review to update the U.S. Preventive Services Task Force recommendations. Ann Intern Med 157 104–113. [PubMed: 22786830]

Nilsson M, Dahlman I, Jiao H, Gustafsson JA, Arner P & Dahlman-Wright K 2007a Impact of estrogen receptor gene polymorphisms and mRNA levels on obesity and lipolysis--a cohort study. BMC Med Genet 8 73. [PubMed: 18053221]

Nilsson M, Dahlman I, Ryden M, Nordstrom EA, Gustafsson JA, Arner P & Dahlman-Wright K 2007b Oestrogen receptor alpha gene expression levels are reduced in obese compared to normal weight females. Int J Obes (Lond) 31 900–907. [PubMed: 17224934]

Nilsson S, Makela S, Treuter E, Tujague M, Thomsen J, Andersson G, Enmark E, Pettersson K, Warner M & Gustafsson JA 2001 Mechanisms of estrogen action. Physiol Rev 81 1535–1565. [PubMed: 11581496]

Ogawa S, Chan J, Gustafsson JA, Korach KS & Pfaff DW 2003 Estrogen increases locomotor activity in mice through estrogen receptor alpha: specificity for the type of activity. Endocrinology 144 230–239. [PubMed: 12488349]

Ohlsson C, Hellberg N, Parini P, Vidal O, Bohlooly YM, Rudling M, Lindberg MK, Warner M, Angelin B & Gustafsson JA 2000 Obesity and disturbed lipoprotein profile in estrogen receptor-alpha-deficient male mice. Biochem Biophys Res Commun 278 640–645. [PubMed: 11095962]

Padilla J, Jenkins NT, Vieira-Potter VJ & Laughlin MH 2013 Divergent phenotype of rat thoracic and abdominal perivascular adipose tissues. Am J Physiol Regul Integr Comp Physiol 304 R543–552. [PubMed: 23389108]

Park YM, Pereira RI, Erickson CB, Swibas TA, Cox-York KA & Van Pelt RE 2017 Estradiol-mediated improvements in adipose tissue insulin sensitivity are related to the balance of adipose tissue estrogen receptor alpha and beta in postmenopausal women. PLoS One 12 e0176446.

Ponnusamy S, Tran QT, Harvey I, Smallwood HS, Thiyagarajan T, Banerjee S, Johnson DL, Dalton JT, Sullivan RD, Miller DD, et al. 2017a Pharmacologic activation of estrogen receptor beta increases mitochondrial function, energy expenditure, and brown adipose tissue. FASEB J 31 266–281. [PubMed: 27733447]

Ponnusamy S, Tran QT, Thiyagarajan T, Miller DD, Bridges D & Narayanan R 2017b An estrogen receptor beta-selective agonist inhibits non-alcoholic steatohepatitis in preclinical models by regulating bile acid and xenobiotic receptors. Exp Biol Med (Maywood) 242 606–616. [PubMed: 28092182]

Qiu S, Vazquez JT, Boulger E, Liu H, Xue P, Hussain MA & Wolfe A 2017 Hepatic estrogen receptor alpha is critical for regulation of gluconeogenesis and lipid metabolism in males. Sci Rep 7 1661. [PubMed: 28490809]

Razmjou S, Bastard JP, Doucet E, Rabasa-Lhoret R, Fellahi S, Lavoie JM & Prud'homme D 2016 Effect of the menopausal transition and physical activity energy expenditure on inflammatory markers: a MONET group study. Menopause 23 1330–1338. [PubMed: 27529462]

Rector RS, Thyfault JP, Morris RT, Laye MJ, Borengasser SJ, Booth FW & Ibdah JA 2008 Daily exercise increases hepatic fatty acid oxidation and prevents steatosis in Otsuka Long-Evans Tokushima Fatty rats. Am J Physiol Gastrointest Liver Physiol 294 G619–626. [PubMed: 18174272]

Ribas V, Nguyen MT, Henstridge DC, Nguyen AK, Beaven SW, Watt MJ & Hevener AL 2010 Impaired oxidative metabolism and inflammation are associated with insulin resistance in ERalpha-deficient mice. Am J Physiol Endocrinol Metab 298 E304–319. [PubMed: 19920214]

Ryan AS, Nicklas BJ & Berman DM 2002 Hormone replacement therapy, insulin sensitivity, and abdominal obesity in postmenopausal women. Diabetes Care 25 127–133. [PubMed: 11772913]

Sasayama D, Sugiyama N, Yonekubo S, Pawlak A, Murasawa H, Nakamura M, Hayashi M, Ogawa T, Moro M, Washizuka S, et al. 2017 Novel oestrogen receptor beta-selective ligand reduces obesity and depressive-like behaviour in ovariectomized mice. Sci Rep 7 4663. [PubMed: 28680060]

Seidlova-Wuttke D, Nguyen BT, Wuttke W. Long-term effects of ovariectomy on osteoporosis and obesity in estrogen-receptor-beta-deleted mice. Comp Med. 2012;62(1):8–13. [PubMed: 22330645]

Shin JH, Hur JY, Seo HS, Jeong YA, Lee JK, Oh MJ, Kim T, Saw HS & Kim SH 2007 The ratio of estrogen receptor alpha to estrogen receptor beta in adipose tissue is associated with leptin production and obesity. Steroids 72 592–599. [PubMed: 17509633]

Sondergaard E, Espinosa De Ycaza AE, Morgan-Bathke M & Jensen MD 2017 How to Measure Adipose Tissue Insulin Sensitivity? J Clin Endocrinol Metab.

Sood R, Faubion SS, Kuhle CL, Thielen JM & Shuster LT 2014 Prescribing menopausal hormone therapy: an evidence-based approach. Int J Womens Health 6 47–57. [PubMed: 24474847]

Stefanska A, Bergmann K & Sypniewska G 2015 Metabolic Syndrome and Menopause: Pathophysiology, Clinical and Diagnostic Significance. Adv Clin Chem 72 1–75. [PubMed: 26471080]

Stubbins RE, Holcomb VB, Hong J & Nunez NP 2012a Estrogen modulates abdominal adiposity and protects female mice from obesity and impaired glucose tolerance. Eur J Nutr 51 861–870. [PubMed: 22042005]

Stubbins RE, Najjar K, Holcomb VB, Hong J & Nunez NP 2012b Oestrogen alters adipocyte biology and protects female mice from adipocyte inflammation and insulin resistance. Diabetes Obes Metab 14 58–66. [PubMed: 21834845]

Thyfault JP, Rector RS, Uptergrove GM, Borengasser SJ, Morris EM, Wei Y, Laye MJ, Burant CF, Qi NR, Ridenhour SE, et al. 2009 Rats selectively bred for low aerobic capacity have reduced hepatic mitochondrial oxidative capacity and susceptibility to hepatic steatosis and injury. J Physiol 587 1805–1816. [PubMed: 19237421]

Tomicek NJ, Lancaster TS & Korzick DH 2011 Increased estrogen receptor beta in adipose tissue is associated with increased intracellular and reduced circulating adiponectin protein levels in aged female rats. Gend Med 8 325–333. [PubMed: 21782527]

Velickovic K, Cvoro A, Srdic B, Stokic E, Markelic M, Golic I, Otasevic V, Stancic A, Jankovic A, Vucetic M, et al. 2014 Expression and subcellular localization of estrogen receptors alpha and beta in human fetal brown adipose tissue. J Clin Endocrinol Metab 99 151–159. [PubMed: 24217905]

Vieira Potter VJ, Strissel KJ, Xie C, Chang E, Bennett G, Defuria J, Obin MS & Greenberg AS 2012 Adipose tissue inflammation and reduced insulin sensitivity in ovariectomized mice occurs in the absence of increased adiposity. Endocrinology 153 4266–4277. [PubMed: 22778213]

Vieira-Potter VJ, Padilla J, Park YM, Welly RJ, Scroggins RJ, Britton SL, Koch LG, Jenkins NT, Crissey JM, Zidon T, et al. 2015 Female rats selectively bred for high intrinsic aerobic fitness are protected from ovariectomy-associated metabolic dysfunction. Am J Physiol Regul Integr Comp Physiol 308 R530–542. [PubMed: 25608751]

Wainright KS, Fleming NJ, Rowles JL, Welly RJ, Zidon TM, Park YM, Gaines TL, Scroggins RJ, Anderson-Baucum EK, Hasty AH, et al. 2015 Retention of sedentary obese visceral white adipose tissue phenotype with intermittent physical activity despite reduced adiposity. Am J Physiol Regul Integr Comp Physiol 309 R594–602. [PubMed: 26180183]

Wang X, Liu J, Long Z, Sun Q, Liu Y, Wang L, Zhang X & Hai C 2015 Effect of diosgenin on metabolic dysfunction: Role of ERbeta in the regulation of PPARgamma. Toxicol Appl Pharmacol 289 286–296. [PubMed: 26408789]

Winn NC, Jurrissen TJ, Grunewald ZI, Cunningham RP, Woodford ML, Kanaley JA, Lubahn DB, Manrique-Acevedo C, Rector RS, Vieira-Potter VJ, et al. 2019 Estrogen receptor-alpha signaling maintains immunometabolic function in males and is obligatory for exercise-induced amelioration of nonalcoholic fatty liver. Am J Physiol Endocrinol Metab 316 E156–E167. [PubMed: 30512987]

Xu Y, Nedungadi TP, Zhu L, Sobhani N, Irani BG, Davis KE, Zhang X, Zou F, Gent LM, Hahner LD, et al. 2011 Distinct hypothalamic neurons mediate estrogenic effects on energy homeostasis and reproduction. Cell Metab 14 453–465. [PubMed: 21982706]

Yamauchi T, Kamon J, Waki H, Terauchi Y, Kubota N, Hara K, Mori Y, Ide T, Murakami K, Tsuboyama-Kasaoka N, et al. 2001 The fat-derived hormone adiponectin reverses insulin resistance associated with both lipoatrophy and obesity. Nat Med 7 941–946. [PubMed: 11479627]

Yan H, Yang W, Zhou F, Li X, Pan Q, Shen Z, Han G, Newell-Fugate A, Tian Y, Majeti R, et al. 2019 Estrogen Improves Insulin Sensitivity and Suppresses Gluconeogenesis via the Transcription Factor Foxo1. Diabetes 68 291–304. [PubMed: 30487265]

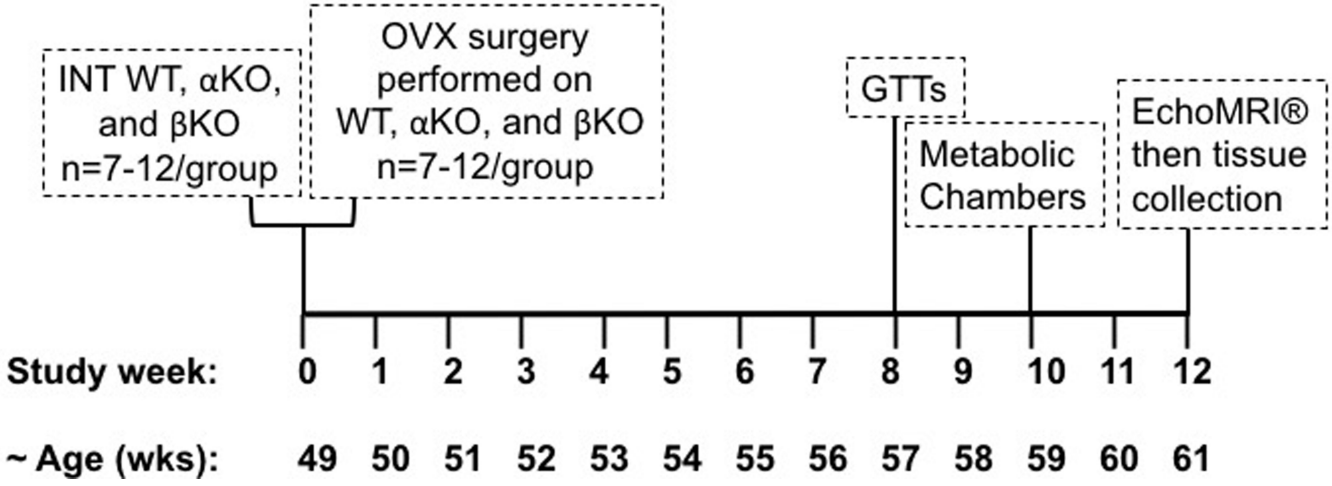


**Figure 1. Overview of study design.**

Wildtype (WT), ERαKO (αKO) and ERβKO (βKO) female mice were either left ovary-intact (INT) or ovariectomized (OVX). INT groups were assessed for all indicated outcomes at 49 wks of age. OVX groups were assessed for body weight and body composition at 49 wks, ovariectomized, then followed for an additional 12 wks and assessed as for all outcomes as indicated above.

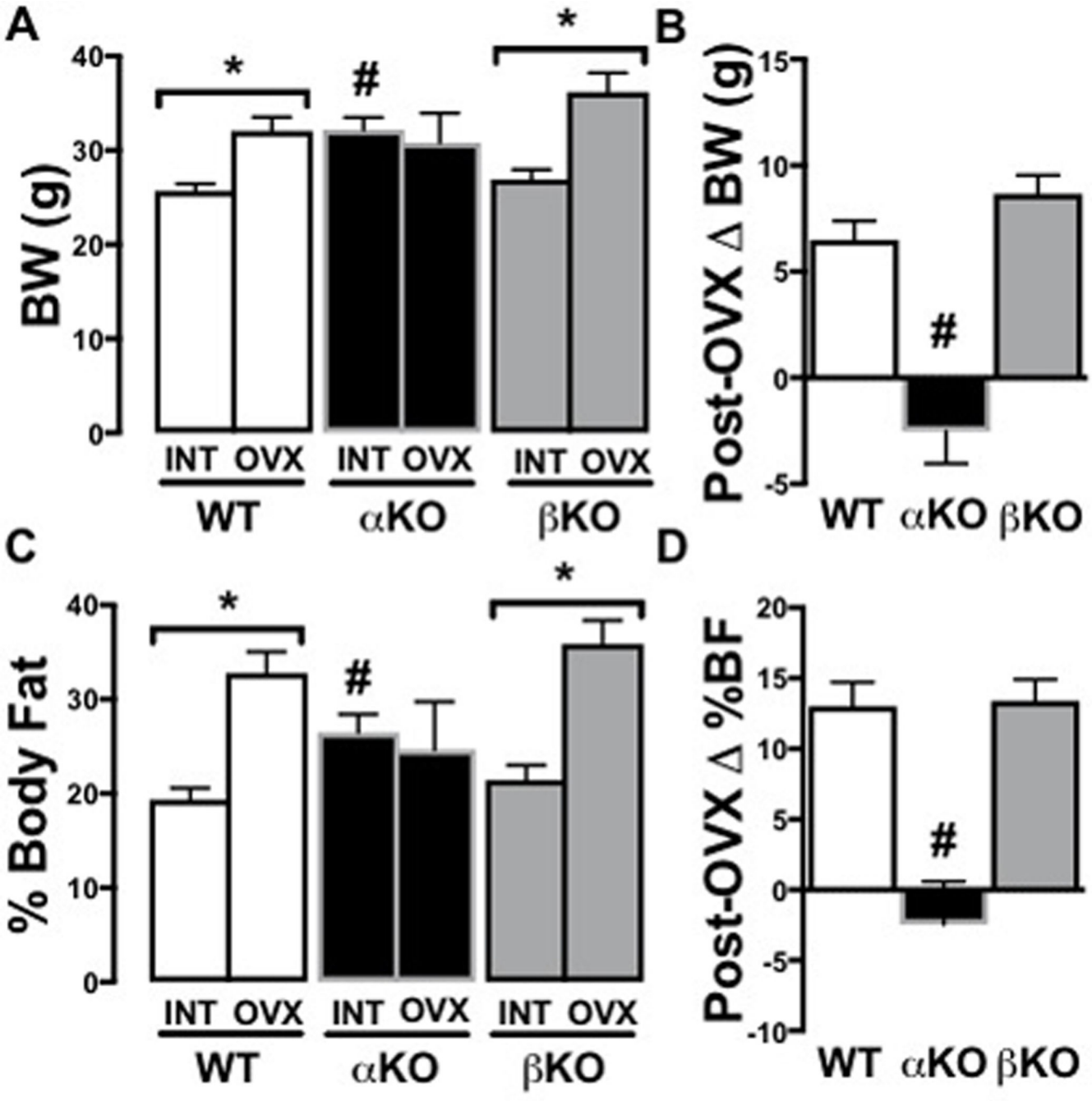


**Figure 2. Genotype-specific body composition changes following ovariectomy.**

(A) Body weight (BW) in INT versus OVX; (B) Change in BW 12 weeks after OVX; (C) % Body fat in INT versus OVX; (D) Change in % body fat 12 weeks after OVX. Ovary-intact (INT); ovariectomized (OVX); wildtype (WT); estrogen receptor alpha knockout (αKO); estrogen receptor beta knockout (βKO). * $p<0.05$ compared to INT within genotype; # $p<0.05$ compared to other genotypes within INT or OVX state. Values are expressed as mean ± SEM.

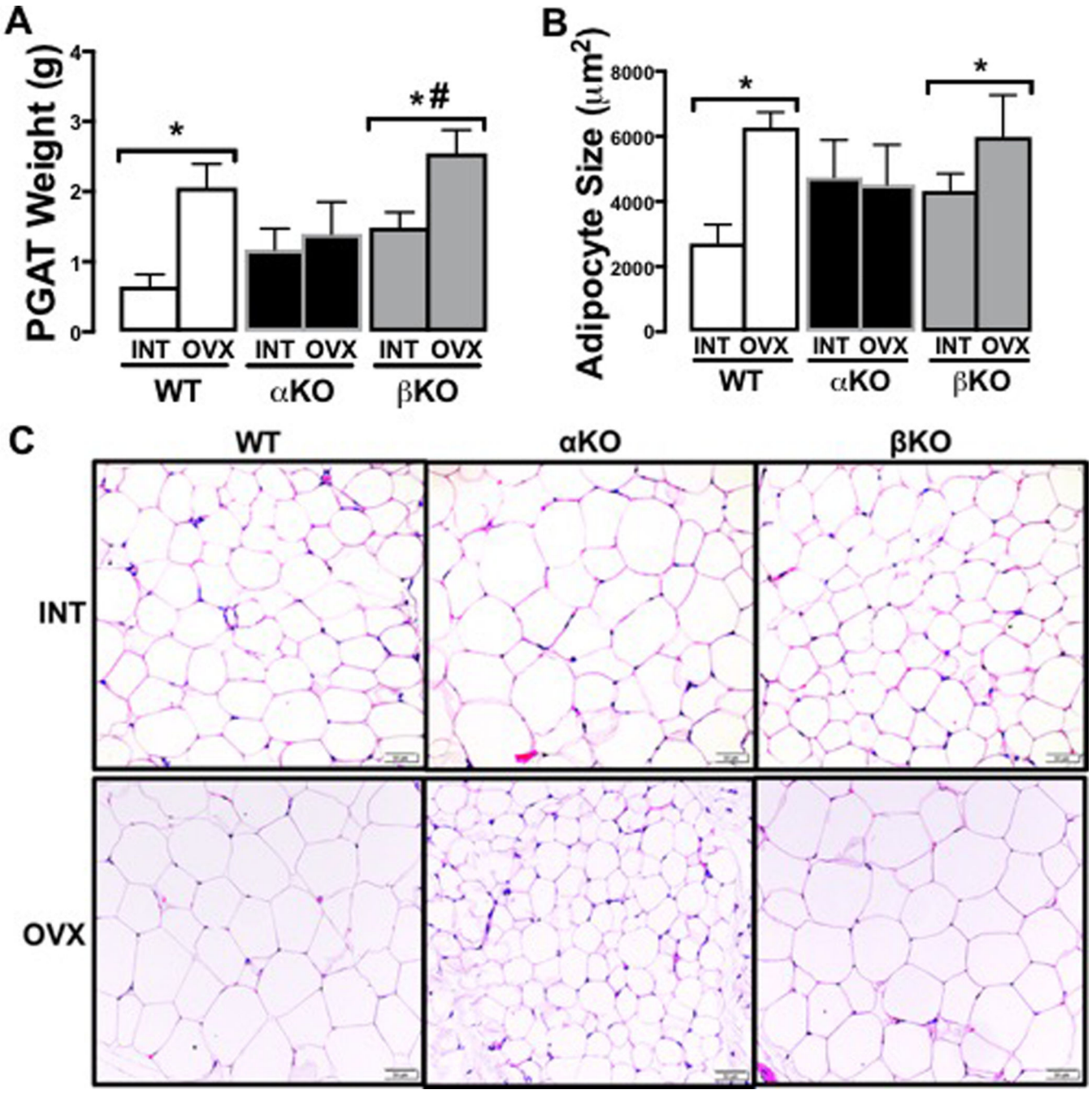


**Figure 3. Genotype-specific visceral adiposity changes following ovariectomy.**

(A) Perigonadal (PGAT) fat pad weights in INT versus OVX; (B) Mean PGAT adipocyte cell size in INT and OVX mice; and (C) Representative histological images of PGAT in INT and OVX mice. Ovary-intact (INT); ovariectomized (OVX); wildtype (WT); estrogen receptor alpha knockout (αKO); estrogen receptor beta knockout (βKO). * $p<0.05$ compared to INT within genotype; # $p<0.05$ compared to αKO within INT or OVX state. Values are expressed as mean ± SEM.

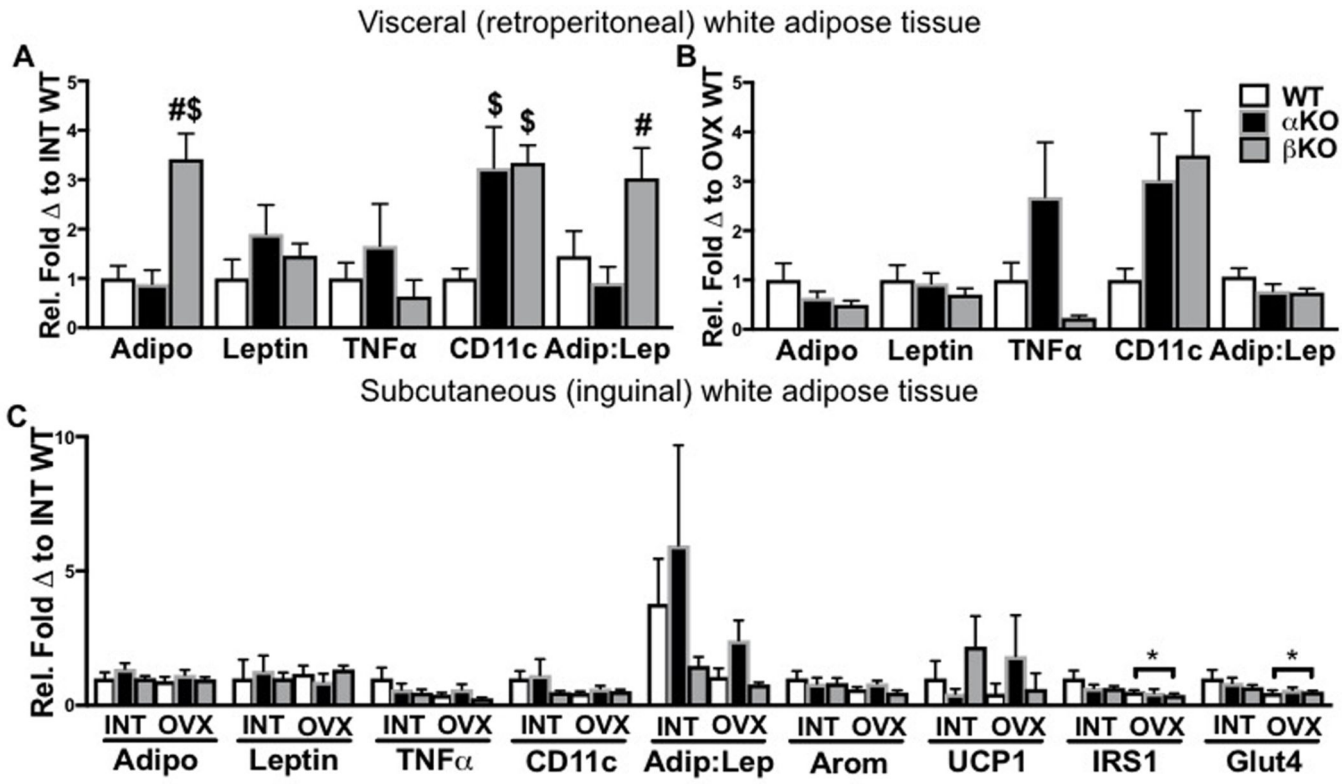


**Figure 4. Genotype-specific differences in white adipose tissue gene expression in intact and ovariectomized states.**

(A) Visceral white adipose tissue (WAT) inflammatory gene expression in ovary-intact (INT) mice; (B) Visceral WAT inflammatory gene expression in ovariectomized (OVX) mice; and (C) Subcutaneous WAT gene expression in INT versus OVX mice. Ovary-intact (INT); ovariectomized (OVX); wildtype (WT); estrogen receptor alpha knockout (αKO); estrogen receptor beta knockout (βKO). * $p<0.05$ compared to INT within genotype; # $p<0.05$ compared to αKO within INT or OVX state; $ $p<0.05$ compared to WT within INT or OVX state. Values are expressed as mean ± SEM.

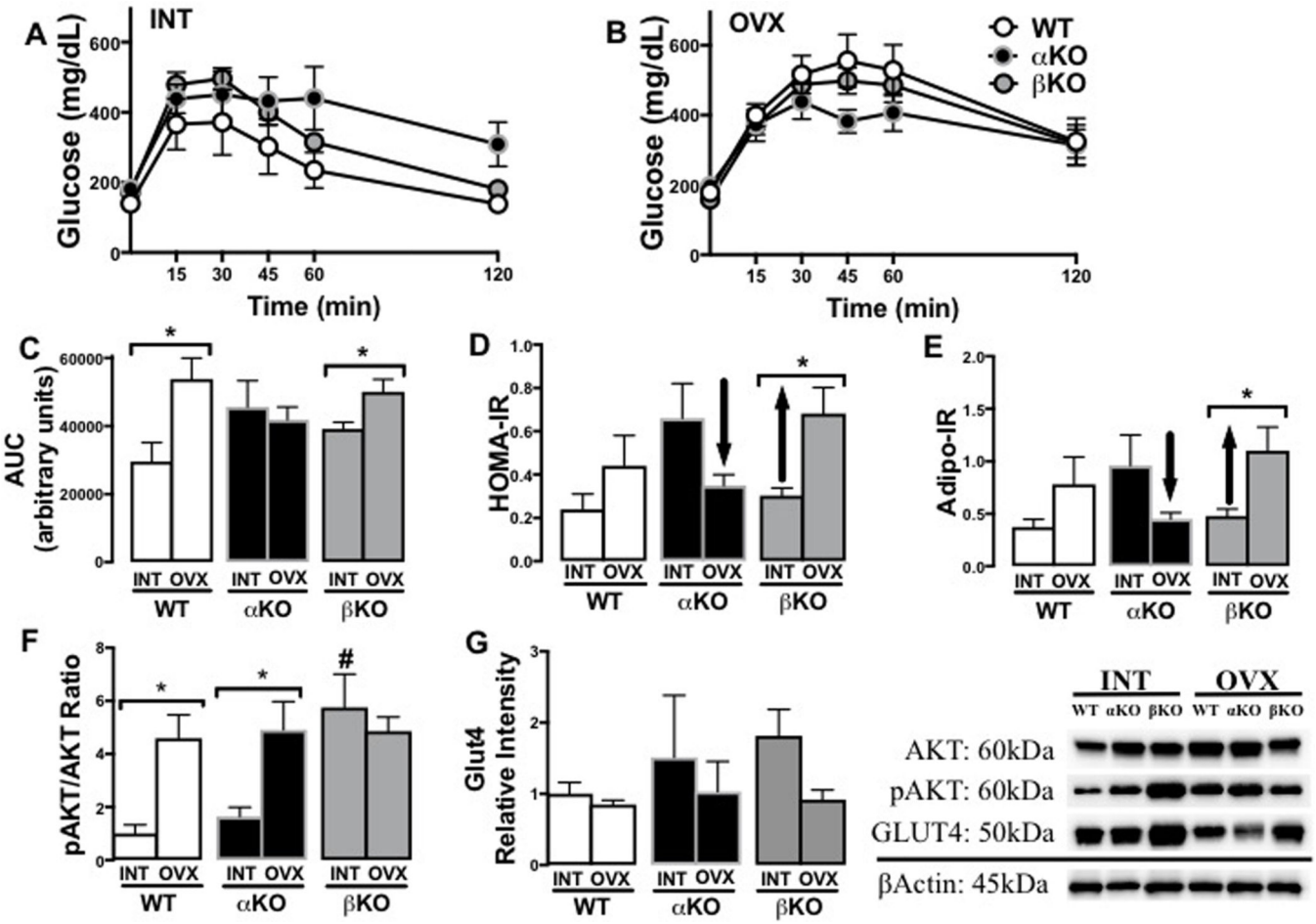


**Figure 5. Genotype-specific changes in indicators of insulin resistance following ovariectomy.**

(A) Glucose tolerance test (GTT) curves of ovary-intact (INT) mice; (B) GTT curves of ovariectomized (OVX) mice; (C) GTT area under the curve (AUC) in INT versus OVX mice; (D) Homeostatic assessment of insulin resistance (HOMA-IR) in INT and OVX mice; (E) Adipocyte insulin resistance (Adipo-IR) in INT and OVX mice; (F) White adipose tissue (WAT) *(from subcutaneous depot)* pAkt/Akt ratio protein levels in INT and OVX mice; and (G) WAT *(from subcutaneous depot)* GLUT4 protein levels in INT and OVX mice *(representative blot images shown to the right)*. Ovary-intact (INT); ovariectomized (OVX); wildtype (WT); estrogen receptor alpha knockout (αKO); estrogen receptor beta knockout (βKO). * $p<0.05$ compared to INT within genotype; # $p<0.05$ compared to other genotypes within INT state. Values are expressed as mean ± SEM.

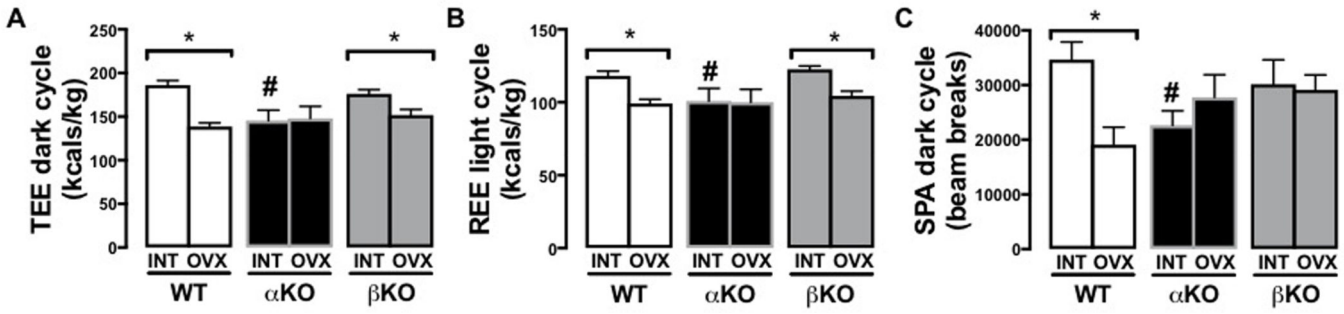


**Figure 6. Genotype-specific changes in energy expenditure and spontaneous physical activity following ovariectomy.**

(A) Total energy expenditure (TEE); (B) Resting energy expenditure (REE); and (C) 12-hr dark cycle spontaneous physical activity (SPA). Ovary-intact (INT); ovariectomized (OVX); wildtype (WT); estrogen receptor alpha knockout (αKO); estrogen receptor beta knockout (βKO); * $p<0.05$ compared to INT within genotype; # $p<0.05$ compared to other genotypes within INT or OVX state. Values are expressed as mean ± SEM.

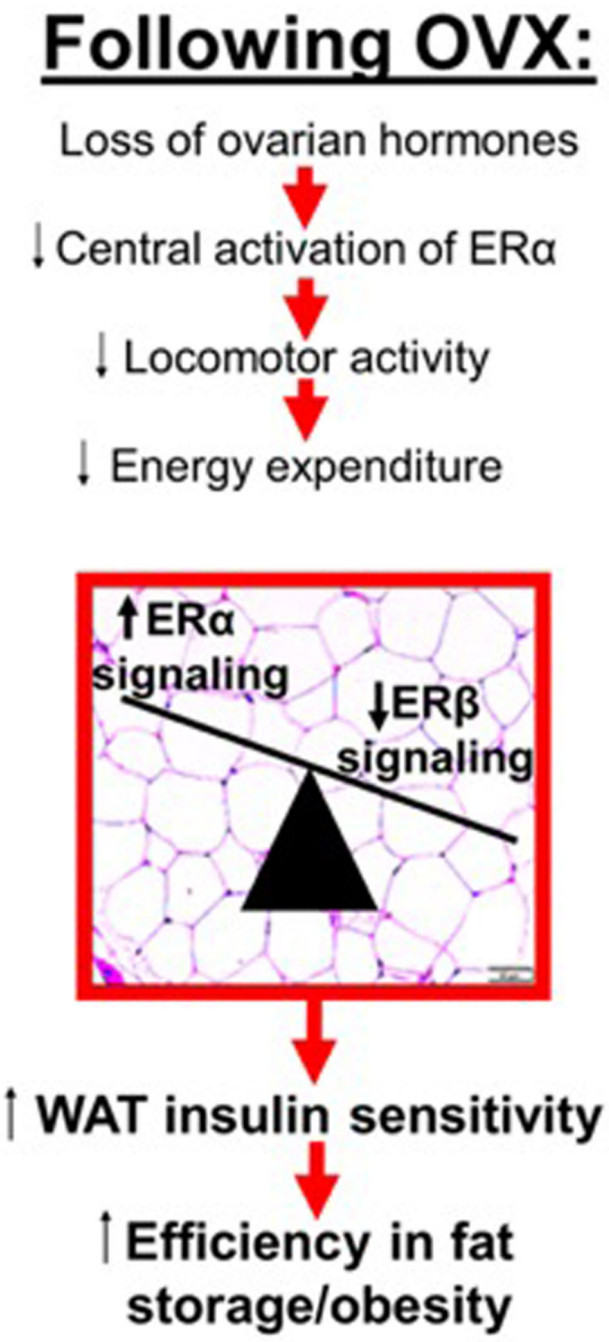


**Figure 7. Proposed model by which a predominance of ERα signaling in white adipose tissue (WAT) may enable ovariectomy (OVX)-induced obesity.**

A greater αKO/βKO ratio favors insulin sensitive WAT creating an obesity phenotype in the setting of low energy expenditure; this is due to increased insulin-mediated lipid deposition. estrogen receptor alpha (ERα); estrogen receptor beta (ERβ).

**Table 1**

q-rtPCR primer sequences

| | 5’−3’ primer sequence forward | 5’−3’ primer sequence reverse | Product Length | NCBI Reference Sequence |
|---|---|---|---|---|
| CD11c | ATGCCACTGTCTGGCTTCAT | GAGCCAGGTCAAAGGTGACA | 84 bp | NM_0213334.3 |
| TNFα | AGCCGATGGGTTGTACCTTG | ATAGCAAATCGGCTGACGGT | 99 bp | NM_013693.3 |
| Adiponectin | GCACTGGCAAGTTCTACTGCAA | GTAGGTGAAGAGAACGGCCTTGT | 122 bp | NM_009605.5 |
| Leptin | CCTATTGATGGGTCTGCCCA | TGAGCGCTACCTGCATAGAC | 95 bp | NM_008493.3 |
| 18s | TCAAGAACGAAAGTCGGAGG | GGACATCTAAGGGCATCAC | 488 bp | NR_003278.3 |

**Table 2.**

**Fasting metabolic parameters and organ weights in ovary-intact (INT) and ovariectomized (OVX) WT, αKO and βKO mice.**

Two (i.e., INT vs OVX) by three (i.e., WT vs αKO vs βKO) ANOVA were performed to determine main effects and interaction effects, which were followed by *post hoc* Tukey's tests where appropriate.

| | WT-INT | WT-OVX | αKO-INT | αKO-OVX | βKO-INT | βKO-OVX |
|---|---|---|---|---|---|---|
| Insulin (ng/mL) | 0.73 ± 0.21 | 0.79 ± 0.17 | 1.29 ± 0.25 | 0.77 ± 0.18 | 0.68 ± 0.08$^{\#}$ | 1.27 ± 0.27$^{\#*}$ |
| Glucose (mg/dL) | 155.7 ± 38.3 | 212.7 ± 29.9 | 219.3 ± 31.8 | 242.9 ± 16.8 | 208.5 ± 14.2 | 213.7 ± 15.8 |
| Cholesterol (mg/dL) | 56.3 ± 7.9 | 62.1 ± 6.4 | 68.7 ± 10.8 | 80.0 ± 6.1 | 74.3 ± 3.5 | 86.4 ± 5.6$^{*\$}$ |
| LDL (mg/dL) | 4.83 ± 1.08 | 5.57 ± 0.90 | 5.14 ± 0.59 | 7.14 ± 1.06 | 4.80 ± 0.20 | 8.80 ± 0.79$^{*\$}$ |
| HDL (mg/dL) | 25.2 ± 2.5 | 32.9 ± 2.8 | 32.1 ± 5.4 | 41.3 ± 2.2 | 34.9 ± 1.3$^{\#}$ | 39.4 ± 2.0$^{*}$ |
| Triglycerides (mg/dL) | 133.5 ± 5.4 | 153.6 ± 9.9 | 133.57 ± 10.0 | 149.3 ± 5.9 | 140.0 ± 5.5 | 148.6 ± 9.3 |
| NEFA (mmol/L) | 0.85 ± 0.15 | 0.88 ± 0.13 | 0.70 ± 0.12 | 0.77 ± 0.07 | 0.74 ± 0.07 | 0.88 ± 0.07 |
| Estradiol (pg/mL) | 13.91 ± 1.76 | 14.22 ± 1.44 | 34.8 ± 11.7$^{\#\$}$ | 9.97 ± 2.45$^{\wedge}$ | 10.0 ± 1.8 | 9.17 ± 2.38 |
| Uterine weight (mg) | 9.17 ± 1.08 | 2.23 ± 0.18$^{*}$ | 8.00 ± 1.62 | 2.44 ± 0.65$^{*}$ | 10.10 ± 1.14 | 4.79 ± 1.24$^{*}$ |
| Liver weight (g) | 1.14 ± 0.12 | 1.12 ± 0.07 | 1.36 ± 0.14 | 1.17 ± 0.13 | 1.27 ± 0.08 | 1.32 ± 0.07 |
| Liver TG (mgTAG/g) | 47.19 ± 7.30 | 36.23 ± 4.99 | 42.40 ± 8.80 | 44.40 ± 10.70 | 77.70 ± 4.43$^{\#}$ | 61.08 ± 9.01$^{\$}$ |

$^{*}$p<0.05;

$^{\wedge}$p<0.06 different from INT within genotype,

$^{\#}$p<0.05 compared to αKO within INT or OVX state;

$^{\$}$p<0.05 different from WT within INT or OVX state. Values are expressed as mean ± SEM.